Physica E 44 (2011) 152–155

Contents lists available at SciVerse ScienceDirect

Physica E

journal homepage: www.elsevier.com/locate/physe

Field emission performances of CNTs bundles array

Jianfeng Dai [a,b,*], Xiaowen Mu [b], Xiaoting Chen [b], Junhong Wang [b], Bi Fu [b]

[a] State Key Laboratory of Gansu Advanced Non Ferrous Metal Materials, Lanzhou 730050, China
[b] School of Science, Lanzhou University of Technology, Lanzhou 730050, China

ARTICLE INFO

Article history:
Received 13 October 2010
Accepted 3 August 2011
Available online 24 August 2011

ABSTRACT

The field emission performances of normal-gate cold cathode, which is composed of different multi-wall carbon nanotubes (MWCNTs) bundles array are calculated. The device parameters such as the arrangement of bundles, array density, gate location, gate voltage, anode voltages and anode–cathode distance affect the field emission properties, which is discussed in detail. The results reveal that the hexagon bundles array needs a lower threshold voltage than square array to reach high field enhancement factor and large emission current density. The emission current density is two orders larger than that of the oxide emitter. The optimal bundles array densities of hexagon and square array to get field enhancement factor are 0.0063 and 0.00375 μm^{-2}, respectively. Meanwhile, the field emission performances are impacted critically by gate location and gate voltage. Field emission properties changed little while the anode–cathode distance varies within tens of micrometers, which increases the process-friendliness of CNTs field emission devices.

1. Introduction

Since the field emission properties of CNTs were discovered in 1995 [1,2], CNTs have become a candidate for field emission. Compared with other field emitters such as spined-type molybdenum field emitter arrays [3], silicon field emission amplifiers [4], diamond micro tip arrays [5] and zinc oxide emitter arrays, CNTs emitter possesses advantages of very high field enhancement factor, low threshold voltage, chemical inertness and thermal stability. Generally, the field enhancement factor of CNTs emitters can reach several thousands while the other emitters' field emission factors do not exceed 600 [6]. Reported results show that CNTs field emitters exhibit excellent field emission properties regardless of morphology, and whether single-walled or multi-walled [7–11]. More important, metal and oxide emitter tip ablate easily at a high temperature and become blunt. Thereby, the field enhancement characters decrease naturally, and its life-span shortens too.

In view of CNTs field emitter (CNTs-FE) possessing excellent field emission property, large area emitter cathode is demanded for CNTs field emission display (CNTs-FED); therefore, it is necessary to make large area CNTs cathode. Many simulations about the field emission performances of single CNT array were reported [12–16]; however, it is difficult to prepare a regularly arranged single CNT array in large scale, while few field emission characters of CNTs bundles array, which could be prepared easily by Chemical Vapor Deposition (CVD) have been calculated. The MWCNTs bundles array normal-gate cathode model has been built in this paper. To make it more convenient for industrial manufacture, the adopted parameters in the paper are based on some experiments [17,18]. Different parameters such as the size of bundles array, array density, anode–cathode distance, gate voltage and the position of normal-gate affect the field emission properties, which include field enhancement factor, emission current density and threshold voltage, which are investigated in this paper.

2. Modeling

2.1. CNTs bundles array cathode

CVD has been shown to be capable of producing vertically pitched MWCNTs, which is useful for field emission applications [19]. The diameters of CNTs in MWCNTs bundles are around 20–30 nm and the lengths range from tens of micrometers to several millimeters. The intertube distance (between two ektexines) is about 10 nm [20–24]. To study the field emission performances of the MWCNTs bundles array cathode with normal-gate, the structural model has been established and a section view is presented in Fig. 1(a). In the model, the anode is made of transparent conductive Indium Tin Oxides (ITO) film with coating of phosphor on the surface. MWCNTs bundles array with a diameter $d_0 = 10$ μm, which is deposited on Si substrate in hexagon

* Corresponding author at: State Key Laboratory of Gansu Advanced Non Ferrous Metal Materials, Lanzhou 730050, China. Tel.: +86 13919078187.
E-mail address: jfdai1963@sohu.com (J. Dai).

1386-9477/$ - see front matter Crown Copyright © 2011 Published by Elsevier B.V. All rights reserved.
doi:10.1016/j.physe.2011.08.006

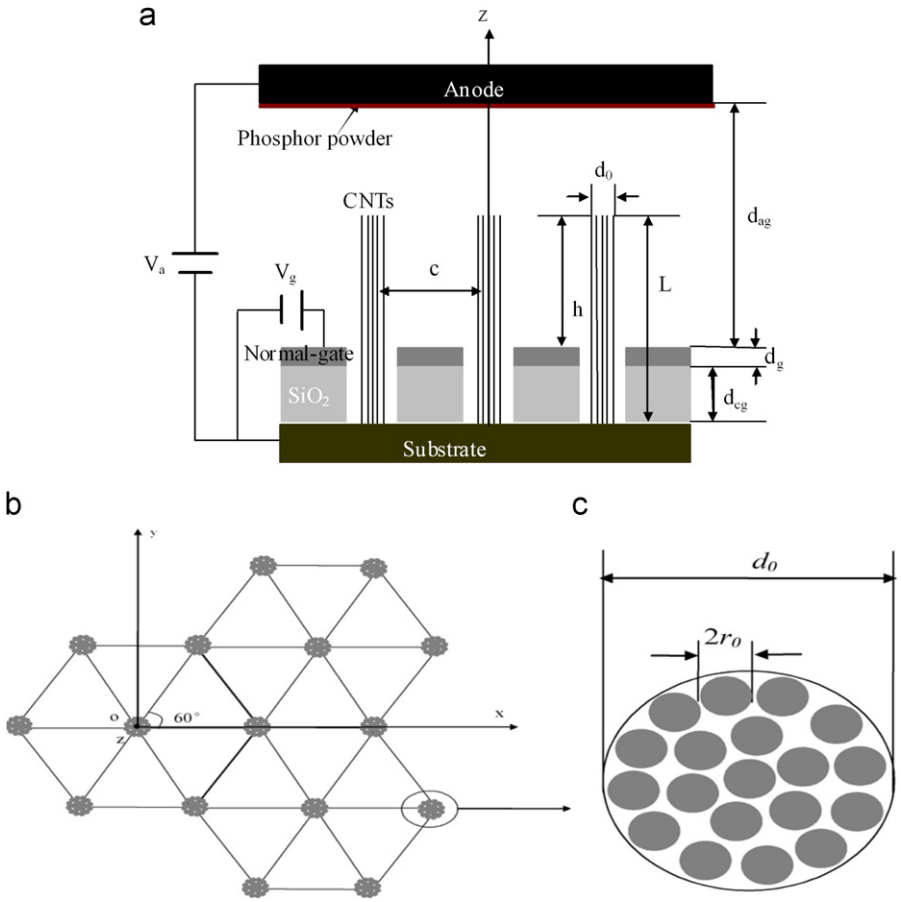

Fig. 1. A schematic plot of the structure: (a) section view, (b) top view and (c) a single bundle. The plots are developed by Jianfeng Dai and Xiaowen Mu.

plays the part of cathode, and the array is photolithographically defined by a mask aligner in this paper [21], as shown in Fig. 1(b) and (c). Evaporation-deposited Al film of thickness d_g=50 nm deposited on silicon dioxide (SiO_2) insulating layer acts as the normal-gate. The anode, cathode and normal-gate are connected with external drive circuit by their own down-leads. The symbol c denotes the space between two neighbored bundles and h is the distance from CNTs top to normal-gate in vertical; d_{ag} and d_{cg} are distances of normal-gate to anode and normal-gate to cathode, respectively. V_a and V_g are anode voltage and normal-gate voltage, respectively. According to some experiments [15,18,19,22], the adopted boundary conditions are V_a=2000 V, V_g=100 V, d_{ag}=100 μm, d_g=50 nm, d_{cg}=30 μm, d_0=10 μm and the cathode plate is grounded. To simplify calculation, assume that all MWCNTs in bundles possess the same size and are perpendicular to the substrate. Those CNTs are cylindrical shape with height L=100 μm, and have been closed with a hemispherical cap with radius r_0=10 nm. It is known that the MWCNTs are metallic and the shielding effect goes into effect when the intertube distance is less than tenfold of CNTs diameter [24,25]. Thus, the bundle can be treated as a metal column, and its potential is maintained to be zero.

2.2. Field emission modeling

In order to build cylindrical coordinates (r,θ,$\boldsymbol{Z}$), the central axes of one bundle and cathode plate are defined as $\boldsymbol{Z}$ axis and xoy plan, respectively, r is the distance from CNTs tip to any point in space. The potential of a single CNT can be described by solving the Laplace equation ($\nabla^2\phi_s$=0). Considering the symmetry, the expression of potential, which is not relevant to angle variable can be expressed as

$$\frac{\partial^2\phi_s}{\partial z^2}+\frac{1}{r}\frac{\partial\phi_s}{\partial r}+\frac{\partial^2\phi_s}{\partial r^2}=0, \tag{1}$$

which is consistent with the former conclusion [13,25–27]. As a result

$$\phi_s(z,r)=V_g+(V_a-V_g)\frac{(z-d_{cg})}{d_{ag}} -\frac{[V_a d_{ag}+(V_a-V_g)(L-d_{cg})]}{d_{cg}e^{k_1(z-L)}(1-e^{-2k_1(d_{ag}+d_{cg}-L)})}(1-e^{-2k_1(d_{ag}+d_{cg}-z)}), \tag{2}$$

where k_1 is a function of r. According to earlier research, electrons of CNTs concentrate on the tip [12,28–29]. As r_0 is far smaller than d_0, the potential of a CNTs bundle ϕ_b can be described as Eq. (3), which based on superposition principle as

$$\phi_b(z,r)=\frac{d_0^2}{4r_0^2}(V_g+(V_a-V_g)\frac{(z-d_{cg})}{d_{ag}} -\frac{V_g d_{ag}+(V_a-V_g)(z-d_{cg})}{d_{ag}N_0(k_1r_0)}N_0(k_1r)). \tag{3}$$

$N_0(k_1r)$ is the zero order Neumann function. In accordance with Ref. [12] and considering the contribution of nearest neighbors' bundles only, the potential and field enhancement factor, respectively of CNTs bundle hexagon array can be expressed as Eqs. (4) and (5):

$$\phi_a(z,r)=\frac{d_0^2}{4r_0^2}(7V_g+7(V_a-V_g)\frac{(z-d_{cg})}{d_{ag}} -\frac{V_g d_{ag}+(V_a-V_g)(z-d_{cg})}{d_{ag}N_0(k_1r_0)}(N_0(k_1r)$$

$$+2N_0(k_1\sqrt{r^2+c^2+rc})+2N_0(k_1\sqrt{r^2+c^2-rc}) +N_0(k_1(r+c))+N_0(k_1(c-r)))), \quad (4)$$

$$\beta=\sqrt{\left(\frac{E_r}{E_0}\right)^2+\left(\frac{E_z}{E_0}\right)^2} =\sqrt{\beta_1^2+\beta_2^2}\ \left(E_r=-\frac{\partial\phi_a}{\partial r},E_z=-\frac{\partial\phi_a}{\partial z},E_0=\frac{V_a-V_g}{d_{ag}}\right). \quad (5)$$

3. Results and discussion

3.1. Relations between field enhancement factor β and array density

The field enhancement factor as a function of array density—the graphics of the function about hexagon and square array, respectively, are presented in Fig. 2(a) and (b). Fig. 2 shows that the field enhancement factor is very sensitive to both array density and gate voltage. It is noticeable that there is an optimal array density to gain the maximum field enhancement factor, which is comparable with single CNTs array. The optimal array densities of hexagon array and square arrays are about 0.0063 and 0.00375 μm^{-2}, respectively. This can be understood by the fact that with increasing bundles array density, the shield effect is strong and the interaction of CNTs bundles is increased. While the array density is too small, the interaction between bundles is worn off and the field enhancement factor is decreased naturally. With increasing gate voltage the field enhancement factor is enlarged, which is in accord with the earlier experiment results [12,30,31]. By comparing Fig. 2(a) and (b), it can be concluded that field enhancement factor of hexagon array is about six times as that of square array and more sensitive to the variety of array density because the hexagon array's coordination number is 3 and the square array's is 1. Moreover, the stability of hexagon close packed (hcp) is superior to that of square array; therefore, normal gated MWCNTs bundles array in hexagon cold cathode field devices will be more practical.

3.2. The variation of β versus d

The influence, which comes from the ratio of the space distance of bundles to the bundle's diameter on enhancement factor is shown in Fig. 3. The curves imply that the field enhancement factor reaches a maximum value at $c/d_0 \approx 2$, which has been reported in the study of single CNT emitters and aligned CNTs array film by several authors [32–35]. The field enhancement factor increases when $c/d_0 < 2$, and reduces sharply when $c/d_0 > 2$. The reasons are that the ratio of c to d_0 affects array density directly and there is an optimal array density to get the maximum enhancement factor. The influence of anode–cathode distance d on field enhancement factor is also shown in Fig. 3. The curves demonstrate that the field enhancement factor keeps the same orders when anode–cathode distance changes to 10 μm. Thus, the manufacturing tolerance of anode is greatly increased and the good processability of CNTs field emission devices is improved.

The relation between field enhancement factor and gate location is studied by fixing the value of c/d_0 as shown in Fig. 4. The results demonstrate that the height of CNTs protruding the normal-gate plays an important role in field emission. When the height is higher, the enhancement factor is larger, which is coincident with that of Ref. [36]. Because the effective aspect ratio of emit tip is risen with increasing height, the field enhancement factor is enlarged with increasing aspect ratio [13–15,28–29].

3.3. Affect of anode voltage V_a to emissions current density J

The ideal field emission current density of CNTs bundle is in accordance with the Fowler–Nordheim (F–N) relation as follows:

$$J=a\phi^{-1}E^2\exp\left[\frac{-b\phi^{3/2}}{E}\right] \quad (6)$$

J is the emission current density (in A/cm^2), $\phi=5$ eV is the work function of MWCNTs in bundle, $a=1.54\times10^{-6}$ A eV V^{-2} and $b=6.83\times10^{-7}$ V eV$^{-3/2}$ cm^{-1} are constants, and E is the excited

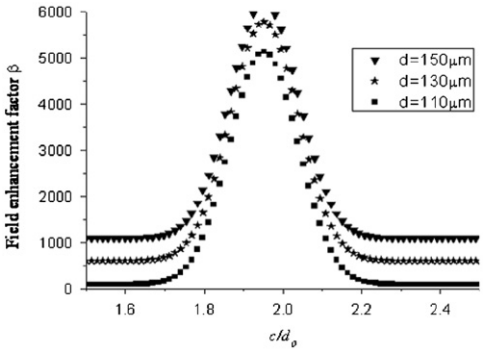

Fig. 3. Relations between β and d, supplied by Junhong Wang.

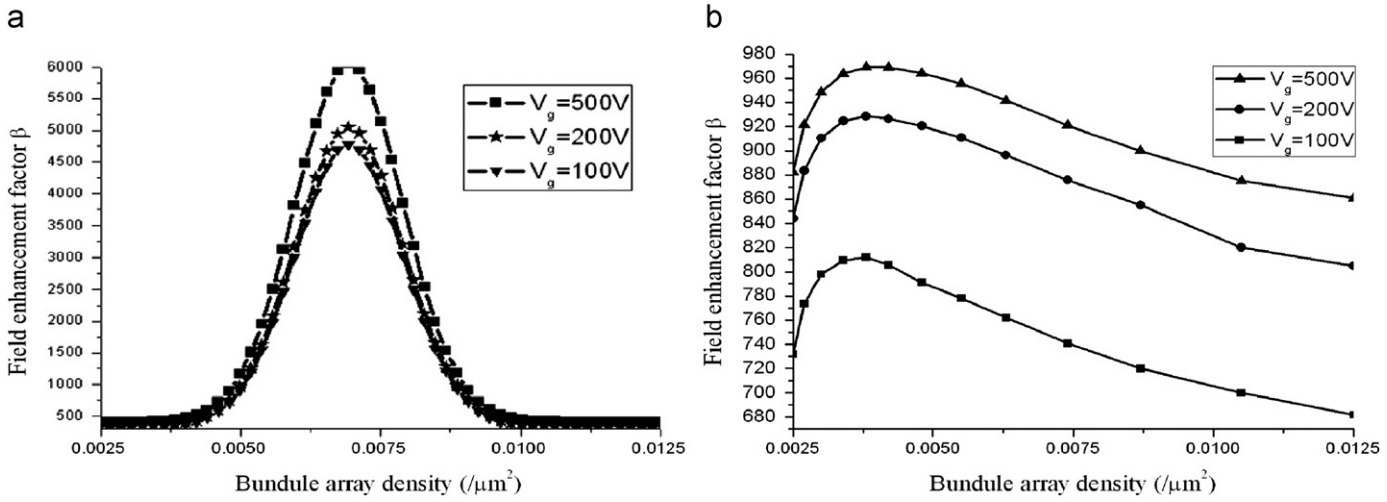

Fig. 2. Field enhancement factor versus CNTs bundle array density: (a) hexagon array and (b) square array, prepared by Xiaowen Mu and Xiaoting Chen.

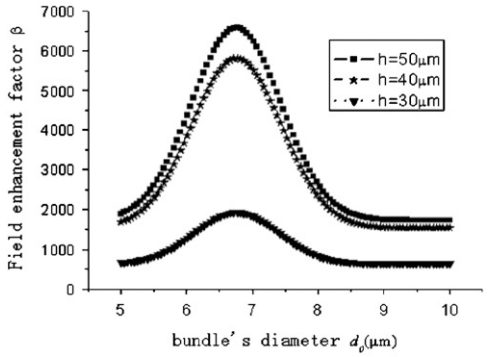

Fig. 4. Relation between β and d_0, supplied by Xiaowen Mu and Bi Fu.

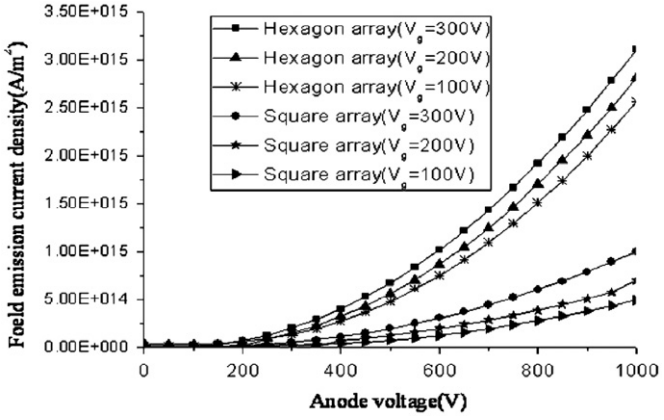

Fig. 5. Emission current density versus anode voltage, prepared by Jianfeng Dai, Xiaowen Mu and Xiaoting Chen.

electric field strength. Emission current density versus anode voltage is plotted in Fig. 5 through varying gate voltages. It is manifest that the emission current density, which is one hundred times larger than that of the oxide emitter, is increased with increasing anode voltage [3–6]; the trends are similar to the experiment results though the value is larger than the experiment results [20,26, 27,31]. The reason is that MWCNTs in bundles are assumed to possess uniform geometric parameters and work function in the model. When the array density is fixed, the higher anode voltage produces a larger local electric field, by which more electrons are migrated from the tip of CNTs to anode plane. The threshold voltage of hexagon CNTs bundles array is decreased by 100 V compared with that of the square array. Emission current density of hexagon array is larger than square array at the same anode voltage. Larger emission current density is excited by higher gate voltage.

4. Conclusion

Field emission properties of MWCNTs bundles array have been calculated and analyzed in this paper. The results are that the field enhancement factor of hexagon bundles array reaches a maximum value at a certain array density, and is much larger than that of square array. The little impact of anode–cathode distance on field enhancement factor improves the commercial feasibility of CNTs field emission devices. Field enhancement factor could be increased by increasing gate voltage and optimizing gate location. Although the field enhancement factor of CNTs bundles array is not increased compared with the single CNTs array, the value is much larger than those of the oxide emitters and sufficient, and CNTs bundles array is easy to realize. Compared with the square array, hexagon array has lower threshold voltage and larger field emission current density, which is about 100 times oxide emitter's. Therefore, field emission characters of MWCNTs bundle with hexagon have a comprehensive prospect of application.

Acknowledgment

The authors gratefully acknowledge the financial support from the National Natural Science Foundation of China (Grant no. 50873047) and Foundation of Gansu Education department of China (Grant no. 0603-02).

References

[1] A.G. Rinzler, J.H. Hafner, P. Nikolaev, L. Lou, S.G. Kim, D. Tomanek, P. Nordlander, D.T. Colbert, R.E. Smalley, Science 269 (1995) 1550.
[2] W.A. de Heer, A. Chatelain, D. Ugarte, Science 270 (1995) 1179.
[3] C.A. Spindt, Surface Science 266 (1992) 145.
[4] M.A.R. Alves, P.H.L. de Faria, E.S. Braga, Microelectronic Engineering 75 (2004) 383.
[5] A. Wisitsora-at, W.P. Kang, J.L. Davidson, M. Howell, W. Hofmeister, D.V. Kerns, Journal of Vacuum Science and Technology B 21 (2003) 614.
[6] W.Z. Chen, S.X. Wang, Y.L. He, Materials Review 23 (2009) 20.
[7] Y.M. Wong, S. Wei, W.P. Kang, J.L. Davidson, W. Hofmeister, J.H. Huang, Y. Cui, Diamond and Related Materials 13 (2004) 2105.
[8] J.M. Bonard, N. Weiss, H. Kind, T. Stöckli, L. Forro, K. Kern, A. Châtelain, Advanced Materials 13 (2001) 184.
[9] Q.H. Wang, T.D. Corrigan, J.Y. Dai, R.P.H. Chang, A.R. Krauss, Applied Physics Letters 70 (1997) 3308.
[10] Z.W. Pan, F.C.K. Au, H.L. Lai, W.Y. Zhou, L.F. Sun, Z.Q. Liu, D.S. Tan, C.S. Lee, S.T. Lee, S.S. Xie, Journal of Physical Chemistry B 105 (2001) 1519.
[11] E. Stratakis, R. Giorgi, M. Barberoglou, Th. Dikonimos, E. Salernitano, N. Lisi, E. Kymakis, Applied Physics Letters 96 (2010) 043110.
[12] J.F. Dai, X.W. Mu, X.W. Qiao, X.T. Chen, J.H. Wang, Chinese Physics B 19 (5) (2010) 057201-1.
[13] Y.B. Zhu, W.L. Wang, K.J. Liao, Acta Physica Sinica 51 (2002) 2335.
[14] M. Luo, X.Q. Wang, H.L. Ge, M. Wang, Y.B. Xu, Q. Chen, L.P. Li, L. Chen, G.F. Guan, J. Xia, F. Jiang, Acta Physica Sinica 55 (2006) 6061.
[15] M. Wang, X.F. Shang, Z.H. Li, Acta Physica Sinica 55 (2006) 797.
[16] W.I. Milne, K.B.K. Teo, G.A.J. Amaratunga, P. Legagneux, L. Gangloff, J.-P. Schnell, V. Semet, V. Thien Binh, O. Groeningd, Journal of Materials Chemistry 14 (2004) 933.
[17] Y.M. Li, T.C. Yeh, Computational Electronics 07 (2008) 332.
[18] Shunjiro Fujii, Shin-ichi Honda, Hironobu Machida, Hideyasu Kawai, Kazuhiro Ishida, Mitsuhiro Katayama, Hiroshi Furuta, Takashi Hirao, Kenjiro Oura, Applied Physics Letters 90 (2007) 876.
[19] C. Bower, W. Zhu, S. Jin, O. Zhou, Applied Physics Letters 77 (2000) 830.
[20] Y.M. Wong, W.P. Kang, J.L. Davidson, B.K. Choi, W. Hofmeister, J.H. Huang, Diamond and Related Materials 14 (2005) 2078.
[21] Y.M. Wong, W.P. Kang, J.L. Davidson, J.H. Huang, D.V. Kerns, Diamond and Related Materials 17 (2008) 552.
[22] D. Kim, S.H. Lim, A.J. Guilley, C.S. Cojocaru, J.E. Bourée, L. Vila b, J.H. Ryu, K.C. Park, J. Jang, Thin Solid Films 516 (2008) 706.
[23] Y.M. Li, H.W. Cheng, Computer Physics Communication 179 (2008) 107.
[24] Z.Q. Fang, M. Hu, H.Y. Li, J.R. Liang, Piezoelectectrics & Acoustooptics 28 (2006) 715.
[25] S.G. Wang, J.H. Wang, Journal of Functional Materials and Devices 08 (2002) 200.
[26] D. Lei, W.B. Wang, L.Y. Zeng, J.Q. Liang, Physica E 41 (2009) 1169.
[27] D. Lei, L.Y. Zeng, Y.X. Xia, S. Chen, J.Q. Liang, W.B. Wang, Acta Physica Sinica 56 (2007) 6616.
[28] X.Q. Wang, M. Wang, H.L. Ge, Q. Chen, Y.B. Xu, Physica E 30 (2005) 101.
[29] J.F. Dai, X.W. Qiao, S.B. Zhang, Q. Wang, W.X. Li, Journal of Functional Materials 11 (2008) 1903.
[30] J.E. Junga, Y.W. Jin, J.H. Choi, Y.J. Park, T.Y. Ko, D.S. Chung, J.W. Kim, J.E. Jang, S.N. Cha, W.K. Yi, S.H. Cho, M.J. Yoon, C.G. Lee, J.H. You, N.S. Lee, J.B. Yoo, J.M. Kim, Physica B 323 (2002) 71.
[31] J.F. Wu, M. Wyse, D. McClain, N. Thomas, J. Jun, Nano Letters 9 (2009) 595.
[32] W.S. Su, F.C. Chuang, T.H. Cho, T.C. Leung, Journal of Applied Physics 106 (2009) 014301-1.
[33] R.C. Smith, D.C. Cox, S.R.P. Silva, Applied Physics Letters 87 (2005) 103112.
[34] Z. Xu, X.D. Bai, E.G. Wang, Applied Physics Letters 88 (2006) 133107.
[35] A.D. Bartolomeo, A. Scarfato, F. Giubileo, F. Bobba, M. Biasiucci, A.M. Cucolo, S. Santucci, M. Passacantando, Carbon 45 (2007) 2957.
[36] Y.K. Li, S.L. Cheng, X.H. Liu, Y.T. Liu, C.C. Zhu, Journal of LiaoNing University 33 (2006) 168.